Limnol. Oceanogr., 50(5), 2005, 1677–1686

Late summer community composition and abundance of photosynthetic picoeukaryotes in Norwegian and Barents Seas

Fabrice Not[1]
Station Biologique, UMR7144 Centre National de la Recherche Scientifique (CNRS), Institut National des Sciences de l'Univers (INSU) et Université Pierre et Marie Curie, Place George Teissier, 29680 Roscoff, France

Ramon Massana and Mikel Latasa
Institut de Ciències del Mar, Consejo Superior de Investigaciones Científicas (CSIC), Passeig Marítim de la Barceloneta 37-49, 08003 Barcelona, Spain

Dominique Marie and Céline Colson
Station Biologique, UMR7144 CNRS, INSU et Université Pierre et Marie Curie, Place George Teissier, 29680 Roscoff, France

Wenche Eikrem
Department of Biology, University of Oslo, P.O. Box 1069 Blindern, 0316 Oslo, Norway

Carlos Pedrós-Alió
Institut de Ciències del Mar, CSIC, Passeig Marítim de la Barceloneta 37-49, 08003 Barcelona, Spain

Daniel Vaulot and Nathalie Simon
Station Biologique, UMR7144 CNRS, INSU et Université Pierre et Marie Curie, Place George Teissier, 29680 Roscoff, France

Abstract

We investigated marine picoeukaryotic diversity (cells <3 μm) in samples collected in late summer 2002 at the boundary between the Norwegian, Greenland, and Barents Seas. The two main Arctic and Atlantic water masses in this region are separated by the polar front. We combined total counts of picoeukaryotes assemblages by flow cytometry and epifluorescence microscopy with taxa detection by tyramide signal amplification–fluorescent in situ hybridization (TSA-FISH) and high performance liquid chromatography (HPLC) pigment analyses. The picoeukaryotic community was primarily composed of photoautotrophs (75% of the cells on average). Members of the division Chlorophyta, in particular the species *Micromonas pusilla* (Butcher) Manton and Parke, were the major components in truly Arctic waters (32% of the picoeukaryotes, maximum 3,200 cells ml^{-1}). *M. pusilla* was also well represented in coastal waters and at the polar front (25% of the picoeukaryotes, maximum 9,100 cells ml^{-1}). Haptophyta were prominent in more typical Atlantic waters (up to 35% of the picoeukaryotes, maximum 4,500 cells ml^{-1}). Quantification of haptophyte biomass by HPLC pigment analyses and CHEMTAX, and haptophyte abundances by TSA-FISH were in good agreement. This confirms previous studies, which suggested that *M. pusilla* is a dominant contributor of picoeukaryotic communities in both coastal and nutrient rich environments, whereas haptophytes seem to be more important in open seawaters.

The Arctic Ocean and adjacent seas are areas of major oceanographic interest because of their contribution to the Atlantic circulation (e.g., deep water formation) and their role in carbon sequestration (Anderson et al. 1998). The area investigated (Fig. 1), at the intersection of the Barents, Norwegian, and Greenland Seas is hydrologically complex and is one of the areas north of 70°N that becomes ice free for some part of the year. Warm and saline Atlantic waters enter from the Norwegian Sea. This North Atlantic current flows northward parallel to the Norwegian coast and then divides into two main branches. One follows the continental slope west of the Spitsbergen archipelago and the other flows eastward into the Barents Sea (Fig. 1). These waters meet less saline and colder Arctic waters flowing southward along the east coast of the Spitsbergen archipelago. The encounter of Atlantic and Arctic water masses around Bear Island forms

[1] To whom correspondence should be addressed. Present address: Marine Microbial Ecology group, Rosenstiel School of Marine and Atmospheric Science, University of Miami, 4600 Rickenbacker Causeway, Miami, Florida 33149-1098 (fnot@rsmas.miami.edu).

Acknowledgments

We wish to thank the F/F *Johan Hjort* crew for efficient assistance with the sampling, as well as the Norwegian Marine Research Institute for providing ship time. Thanks are also due to Francisco Rodriguez for help with CHEMTAX analysis and helpful discussion. We thank Connie Lovejoy and Alexandra Worden for critically reading this manuscript and two anonymous reviewers for helpful comments and suggestions. This work was funded by the following programs: PICODIV supported by the European Union (EVK3-CT-1999-00021), PICMANCHE supported by the Région Bretagne, and the Biogeochemistry and Optic South Pacific Experiment (BIOSOPE) supported by Processus Biogéochimiques dans l'Océan et Flux (PROOF), CNRS. F.N. was supported by a doctoral fellowship from the French Research Ministry.

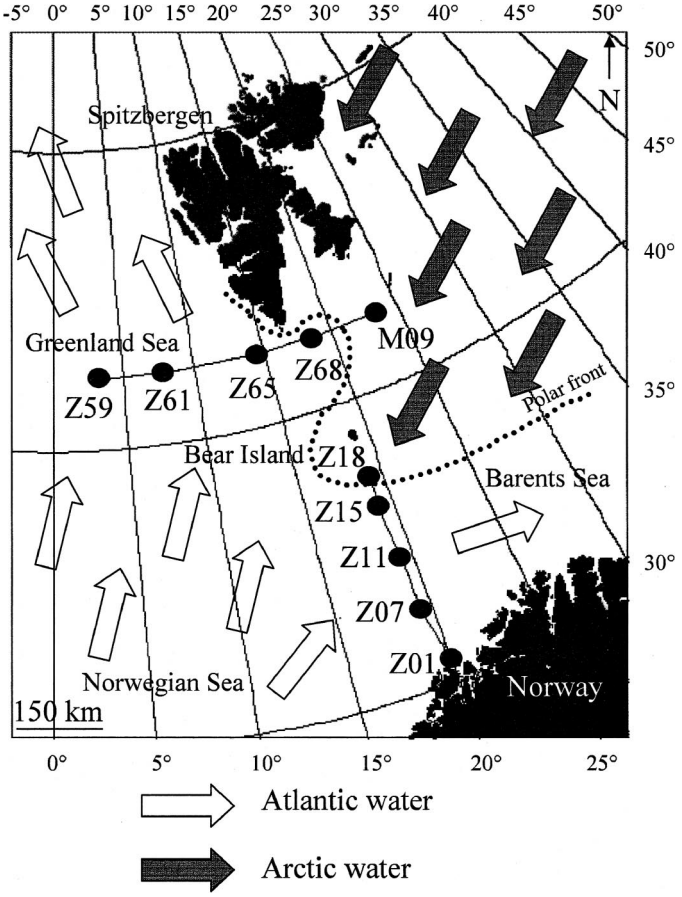

Fig. 1. Map of the cruise area. The two transects S/N (south/north) and E/W (east/west) are indicated. Arrows represent surface circulation and origin of waters encountered, adapted from Markowski and Wiktor (1998).

a marked polar front. The exact position of this front varies with time.

The Barents Sea shelf is one of the most biologically productive regions of the world. In the waters of Atlantic origin, a phytoplankton bloom develops in May–June while post-bloom communities are observed in summer (Kogeler and Rey 1999). Although large interannual variations in the timing of the bloom are observed in the northern Barents Sea (Arctic waters), it usually starts earlier, in April–May immediately after the ice starts melting (Kogeler and Rey 1999). In the region we investigated, diatoms make up typically most of the microphytoplankton species inventories, while dinoflagellates as well as flagellates such as *Phaeocystis pouchetii* (Hariot) Lagerheim and cryptophytes have also been reported in significant numbers (Markowski and Wiktor 1998; Rat'kova et al. 1998). In contrast, there have been few studies focused on the picophytoplankton (cells <3 μm) in Arctic waters. Murphy and Haugen (1985) found that the cyanobacterium *Synechococcus* Nägeli decreases in abundance with increasing latitude. Verity et al. (1999) and Rat'kova and Wassmann (2002) observed that total chlorophyll biomass is dominated by small flagellates and monads during periods outside microphytoplankton blooms (respectively in the Barents Sea and off northern Norway). Throndsen (1970) noted that green flagellates related to the class Prasinophyceae were significantly represented and that the prasinophyte species *Micromonas pusilla* was very abundant in this area.

Here we examined the diversity and abundance of eukaryotic picophytoplankton in relation to hydrological features along two transects through the complex region around the polar front located between the Norwegian and Barents Seas. Samples were collected in late summer, when the overall contribution of picophytoplankton to total phytoplankton was expected to be large. The combined use of pigment analyses, tyramide signal amplification–fluorescent in situ hybridization (TSA-FISH) with oligonucleotide probes, epifluorescence microscopy, and flow cytometry (FCM) allowed us to investigate the importance of eukaryotic picoplankton and to identify the main phylogenetic groups within this complex assemblage.

Material and methods

Sampling procedures—Sampling was done during an oceanographic cruise on board the F/F *Johan Hjort* (Norwegian Institute of Marine Research). This cruise took place in an area between the Norwegian, Greenland, and Barents Seas (Fig. 1). Ten stations were sampled from 20 August to 8 September 2002 along two transects (south/north, S/N and east/west, E/W) south of the Spitsbergen archipelago (Fig. 1 and Table 1). Samples were collected at five depths with a conductivity–temperature–depth (CTD) rosette system equipped with Niskin bottles (5 liters). Chlorophyll fluorescence provided by a SD200W fluorometer was used as a guide to choose the five sampling depths: in the mixed layer (5 m), just above the chlorophyll maximum (ca. 10 m), chlorophyll maximum, just below the chlorophyll maximum (ca. 10 m), and below the euphotic zone (60 m). Water was prefiltered through a 200-μm mesh to remove zooplankton, large phytoplankton, and particles before further filtrations.

DAPI staining—Microbial counts were performed on board with a Zeiss epifluorescence microscope. Glutaraldehyde (Sigma) fixed samples (20 ml, 1% glutaraldehyde final concentration) were stained with 4′6-diamidino-2-phenylindole (DAPI, 5 μg ml^{-1} final concentration) and filtered through 0.6-μm black, 25-mm diameter polycarbonate filters (Poretics). Flagellates were identified and counted by standard epifluorescence microscopy (Porter and Feig 1980) based on their blue fluorescence under ultraviolet (UV) excitation (360 nm). The presence or absence of chlorophyll in flagellates was determined based on their red fluorescence under blue light excitation (490 nm). The size of each individual cell was estimated using an ocular grid in order to obtain the abundances of cells for three size classes (2, 3–4, and 5 μm). Total flagellate counts were grouped into categories based on size and presence or absence of chloroplasts.

Flow cytometry—Samples for flow cytometry were prefiltered through a 3-μm Nuclepore filter (Whatman). Then 1.5 ml of seawater was fixed with a mixture of 1% paraformaldehyde (PFA) and 0.1% glutaraldehyde (final concentra-

Table 1. Position, bottom depth, and hydrology for each sampling station.

Station	Latitude	Longitude	Bottom depth (m)	Chlorophyll max* (ng L^{-1})	Depth of chlorophyll max (m)	Surface temperature (°C)	Surface salinity
Z01	70°30′	20°04′	155	650	13	12.6	33.26
Z07	71°30′	19°48′	234	1,320	25	11.9	34.41
Z11	72°31′	19°36′	390	1,249	25	11.0	34.56
Z15	73°29′	19°18′	479	1,323	16	8.9	34.86
Z18	73°59′	19°14′	128	1,701	6	4.5	34.31
M09	76°19′	23°45′	67	1,835	20	4.5	34.39
Z68	76°20′	18°47′	268	1,393	5	7.1	34.11
Z65	76°20′	14°53′	354	1,674	16	7.1	34.88
Z61	76°20′	7°60′	2,170	891	16	8.2	35.05
Z59	76°20′	3°59′	3,231	737	36	6.0	33.63

* Chlorophyll max, maximum of Chlorophyll *a* concentration.

tion), frozen in liquid nitrogen, and stored at −80°C. Total photosynthetic cell counts were obtained using a FACSsort flow cytometer (Becton Dickinson) following the protocol described by Marie et al. (1999). Photosynthetic picoeukaryotes were discriminated from cyanobacteria and enumerated using Cytowin software available from http://www.sb-roscoff.fr/Phyto/ (Vaulot 1989).

Pigment analyses—Three size fractions were collected: <200 μm onto GF/F filters (Whatman), 3–200 μm onto 3-μm pore size polycarbonate filters (Nuclepore) and <3 μm onto GF/F filters (0.7-μm pore size). One liter of seawater was filtered under a pressure of 200 mm Hg for each of the size fractions. Filters were immediately frozen in liquid nitrogen then subsequently stored at −80°C. High performance liquid chromatography (HPLC) pigment analyses were performed following Zapata et al. (2000) with minor modifications as described in Latasa et al. (2001). The contribution of different algal groups to total chlorophyll *a* (Chl *a*) was estimated using CHEMTAX (Mackey et al. 1996). The HPLC data provided total Chl *a* abundance for each size fraction analyzed. It should be noted that CHEMTAX groups did not exactly match a single taxonomic entity. Thus, each pigment group corresponded to a certain pigment signature that could incorporate contributions from several taxa. The pigment interpretation of the three CHEMTAX groups included in this study is as follows. DIAT_HPLC refers to fucoxanthin-containing groups, mainly members of the Bacillariophyceae (diatoms), but also including other heterokonts (Chrysophyceae, Pelagophyceae, Dictyochophyceae, and Bolidophyceae), and haptophytes. The output pigment : Chl *a* ratios used to estimate the contribution of each phytoplankton groups in the surface (above the deep chlorophyll maximum) and deep samples were, respectively: fucoxanthin 0.421 and 0.361; Chl c_2 0.187 and 0.095; and Chl c_1 0.024 and 0.022. GREEN_HPLC refers to Chl *b* containing organisms (i.e., green algae) such as *M. pusilla* and *Bathycoccus prasinos* Eikrem and Throndsen, for instance. The output pigment : Chl *a* ratios were prasinoxanthin 0.230 and 0.239; neoxanthin 0.074 (both layers); and Chl *b* 0.269 and 0.243. Finally, HAPTO_HPLC are defined by the presence of both 19′hexanoyloxyfucoxanthin (19′hex) and fucoxanthin, a pigment pattern representative of genera such as *Emiliania* Hay and Mohler, *Phaeocystis* Lagerheim, and *Chrysochromulina* Lackey. The output pigment : Chl *a* ratios used were fucoxanthin 0.676 and 0.398; 19′-hexanoylfucoxanthin 0.653 and 0.384; Chl c_3 0.339 and 0.221; and Chl c_2 0.199 and 0.177.

TSA-FISH—For whole cell TSA-FISH, 90 ml of seawater were prefiltered through a 3-μm pore size polycarbonate filter at low pressure (100 mm Hg), fixed with 10 ml of 10% PFA, and kept at 4°C for 1 h. Samples were then filtered onto 0.2-μm Anodisc filters (Whatman) under a maximum pressure of 200 mm Hg and dehydrated in an ethanol series (50%, 80%, 100%, 3 min each). Filters were stored at −80°C. Labeling of probes with horseradish peroxidase (HRP), hybridization conditions, signal amplification, and target cell detection were performed as described in Not et al. (2002). The probes used in this study are listed in Table 2 and are available at the rRNA probe database for protists and cyanobacteria (http://www.sb-roscoff.fr/Phyto/Databases/RNA_probes_introduction.php). Since no unique probe exists to target the whole Eukaryota lineage (any single probe has mismatches to many eukaryotes), we used a combination of three probes with a broad specificity, as described in Not et al. (2004) and Not et al. (2002): EUK 1209R, which has been designed to target all eukaryotes, and CHLO01 and NCHLO01, which have been designed to label Chlorobionta and all other eukaryotes, respectively. Probe CHLO02 was used to target cells belonging to the division Chlorophyta (Not et al. 2004). The other probes target algal orders or classes (PRAS04, PRYM02, and BOLI02) or particular genera within prasinophytes (MICRO01, BATHY01, and OSTREO01). Hybridized cells were observed with an Olympus BX51 epifluorescence microscope (Olympus Optical Co.) equipped with a mercury light source and a 100× UVFL objective. Excitation/emission filters were 360/420 for DAPI and 490/515 for fluorescein isothiocyanate, FITC. For each sample 15 randomly chosen microscopic fields were analyzed and counted manually. For probes with a broad taxonomic specificity (e.g., CHLO02), more than 500 cells were counted.

Data representation using Ocean Data View software—Contour maps showing the parameter distributions are presented using Ocean Data View software (Schlitzer 2003).

Table 2. List of oligonucleotide probes used in this study. The probes EUK1209R, CHLO01, and NCHLO01 were used together in order to target all eukaryotes.

Probe	Sequence	Target group	References
EUK1209R	5′-GGG CAT CAC AGA CCT G-3′	Eukaryotes*	Giovannoni et al. (1988)
CHLO01	5′-GCT CCA CGC CTG GTG GTG-3′	Chlorophyta*	Simon et al. (1995)
NCHLO01	5′-GCT CCA CTC CTG GTG GTG-3′	Non-Chlorophyta*	Simon et al. (1995)
CHLO02	5′-CTT CGA GCC CCC AAC TTT-3′	Chlorophyta*	Simon et al. (2000)
PRAS04	5′-CGT AAG CCC GCT TTG AAC-3′	Mamiellales	Not et al. (2004)
MICRO01	5′-AAT GGA ACA CCG CCG GCG-3′	*Micromonas*	Not et al. (2004)
BATHY01	5′-ACT CCA TGT CTC AGC GTT-3′	*Bathycoccus*	Not et al. (2004)
OSTREO01	5′-CCT CCT CAC CAG GAA GCT-3′	*Ostreococcus*	Not et al. (2004)
PRYM02	5′-GGA ATA CGA GTG CCC CTG AC-3′	Haptophyta	Simon et al. (2000)
BOLI02	5′-TAC CTA GGT ACG CAA ACC-3′	Bolidophyceae	Guillou et al. (1999)

* The specificity of the probes EUK1209R, CHLO01, NCHLO01, and CHLO02 has been revised in Not et al. (2002) and Not et al. (2004).

The shape of contour lines results from computer interpolation. Therefore, features in the plots and their positions must be considered in relation to the frequency and proximity of sampling locations and depths.

Results

Water masses—Hydrological parameters (temperature and salinity) along the S/N and E/W transects enabled us to distinguish waters of Arctic origin (Stas. Z18 and M09) from North Atlantic current waters (Stas. Z01 to Z15 and Stas. Z59 to Z68) (Fig. 1). The Arctic water, flowing down through the east Spitsbergen and Barents Sea, was characterized by low temperatures (range 1.7°C to 4.7°C) and low salinities (ca 34.5) (Fig. 2A,B and Table 1). These moderately stratified waters showed high surface concentration of total and picoplanktonic Chl *a* (>1,400 ng L^{-1} and >800 ng L^{-1}, respectively) (Fig. 2C). Since *Synechococcus* cyanobacteria were absent from these waters (Fig. 2E), essentially all picoplanktonic Chl *a* derived from eukaryotic cells.

The Atlantic-influenced waters were characterized by higher surface temperatures (>6°C) and salinities generally above 34.5 (Fig. 2A,B and Table 1). Total and picoplanktonic Chl *a* concentrations were lower (<1,200 ng L^{-1} and <500 ng L^{-1}, respectively), and *Synechococcus* was always present. Stratification was more pronounced with a mixed layer depth of about 20 m. Within these Atlantic waters, differences between stations were identified. Station Z01 presented coastal features with low salinity at surface and high *Synechococcus* abundance (around 25,000 cells ml^{-1}) (Fig. 2B,E). The low temperature and salinity at Sta. Z59 probably indicate the influence of Arctic waters flowing south along the east coast of Greenland and directed eastward by one of the Greenland Sea gyres. Stations Z65 and Z68 (E/W transect), at the intersection of the Arctic and Atlantic waters (Polar front), exhibited intermediate temperatures, salinities, Chl *a* concentrations, and *Synechococcus* abundances (Fig. 2). Stations Z11 and Z15, close to the polar front, were slightly warmer and saltier (Fig. 2A,B). Additionally, the higher *Synechococcus* densities observed at these stations compared with Stas. Z65 and Z68 suggest a more pronounced influence of coastal and Atlantic waters. Overall stations of the S/N transect appeared more influenced by waters of Atlantic origin and stations of the E/W transect by waters from Arctic origin.

Contribution of picoplankton to photosynthetic biomass—Size fractionated HPLC pigment analyses showed that on average 44% of the Chl *a* biomass could be attributed to picophytoplankton (including *Synechococcus* and picoeukaryotes) in the region studied. At stations influenced by Arctic (Z18 and M09) and coastal (Z01 and Z07) waters, picoplankton represented on average 73.5% and 45% of total Chl *a* biomass, whereas at the polar front and at stations influenced by Atlantic waters (Z11, Z15, Z68, Z65, Z61) their contribution was lower (average 33.5%) (Fig. 2D).

Contribution of different algal groups by pigment analysis—The CHEMTAX program was used to interpret the HPLC data and determine the contribution of the different pigment groups within the picoplanktonic fraction (Fig. 3). The two groups better represented by specific pigments (i.e., diatoms and haptophytes) determined the pattern of picoplanktonic Chl *a* concentrations. The DIAT_HPLC pigment group was particularly abundant in Arctic waters where it represented on average 83% of picoplanktonic Chl *a* (maximum up to 1,300 ng Chl *a* L^{-1}) compared with 31% on average in other water masses. The HAPTO_HPLC pigment type also contributed significantly to the picoplanktonic Chl *a* biomass with 8% and 35% in Arctic and other water masses, respectively (maximum 125 ng Chl *a* L^{-1}, Fig. 3B). The highest concentrations of Chl *a* attributed to HAPTO_HPLC occurred between 20 and 30 m depth in Atlantic waters of both transects, and significant concentrations were observed at Arctic Sta. Z18 (Fig. 3B). By contrast, HAPTO_HPLC were scarce at the coastal influenced Sta. Z01 and at Arctic Sta. M09. The Chl *a* attributed to GREEN_HPLC was always below 50 ng Chl *a* L^{-1}, with highest values around 30 m in the S/N transect and at surface for Arctic-influenced stations (E/W transect) (Fig. 3C).

Abundance of picoeukaryotes—We estimated the overall abundance of picoeukaryotes (both photosynthetic and heterotrophic) by epifluorescence microscopy of DAPI-stained cells. On average, 75% of the cells observed under microscopy were photosynthetic, as determined by the presence of

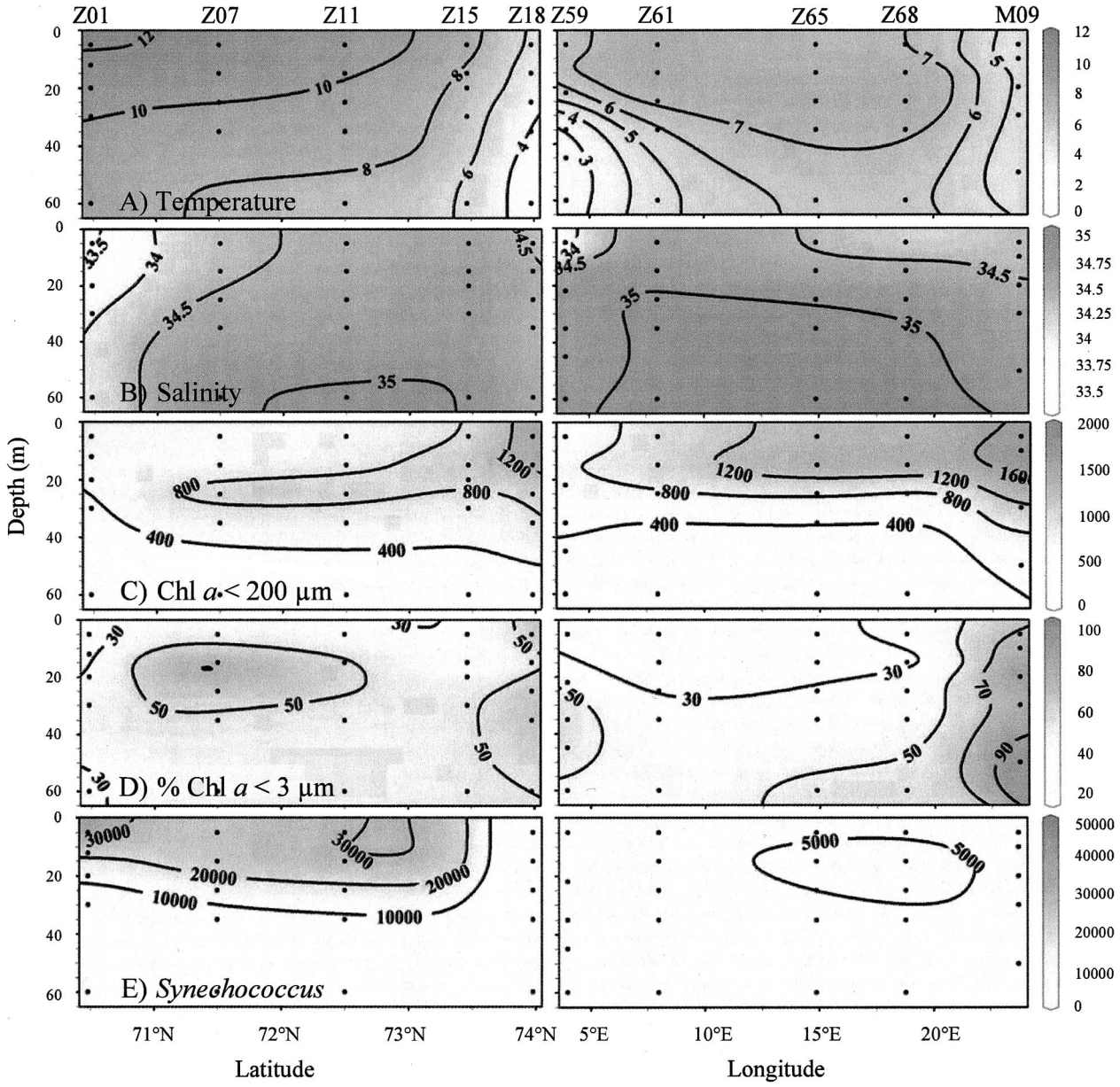

Fig. 2. Depth sections along the S/N and E/W transects. (A) Temperature (°C). (B) Salinity. (C) Chl $a < 200$ μm (ng L^{-1}). (D) Contribution of picoplanktonic Chl a (<3 μm) to Chl $a < 200$ μm (%) (E) *Synechococcus* (cells ml^{-1}). Black dots correspond to actual samples.

chlorophyll. The DAPI counting allowed us to differentiate organisms based on cell size or a conspicuous morphology. Thus, within the photosynthetic eukaryotes, separate counts were performed for very small cells (<2 μm) with a single chloroplast, cells of 3–4 μm that displayed generally two lateral chloroplasts, cells of 5 μm or larger, cryptomonads, and diatoms. In all samples, the average abundance of these cell classes was 58%, 30%, 5%, 1%, and 6% respectively. Among them, the picophytoplankton fraction (collected after a 3-μm filtration) corresponded to cells of 2 μm, cells of 3–4 μm, and the diatoms, since most observed diatoms were very thin (width less than 2 μm and length of 8–10 μm). The average contribution of these three classes of picoeukaryotes to biovolume assuming simple cell shapes would be 21% (cells <2 μm), 67% (cells 3–4 μm), and 12% (thin diatoms) (data not shown).

Total counts of picoeukaryotes were also done by using TSA-FISH with a mix of general eukaryotic probes (Fig. 4A). Both DAPI and FISH counts showed a similar pattern for the distribution of picoeukaryotes, and quantifications were in agreement ($r^2 = 0.89$, $p < 0.001$, $n = 45$, $y = 0.88x - 318$). Enumeration of photosynthetic picoeukaryotes by FCM (Fig. 4B) and based on DAPI counts were also in agreement ($r^2 = 0.95$, $p < 0.001$, $n = 45$, $y = 1.2x + 250$). Stations of the E/W transect presented higher abundances compared with stations of the S/N transect, but in all the measured transects, abundance of picoeukaryotes beyond 4,000 cells ml^{-1} was always restricted to

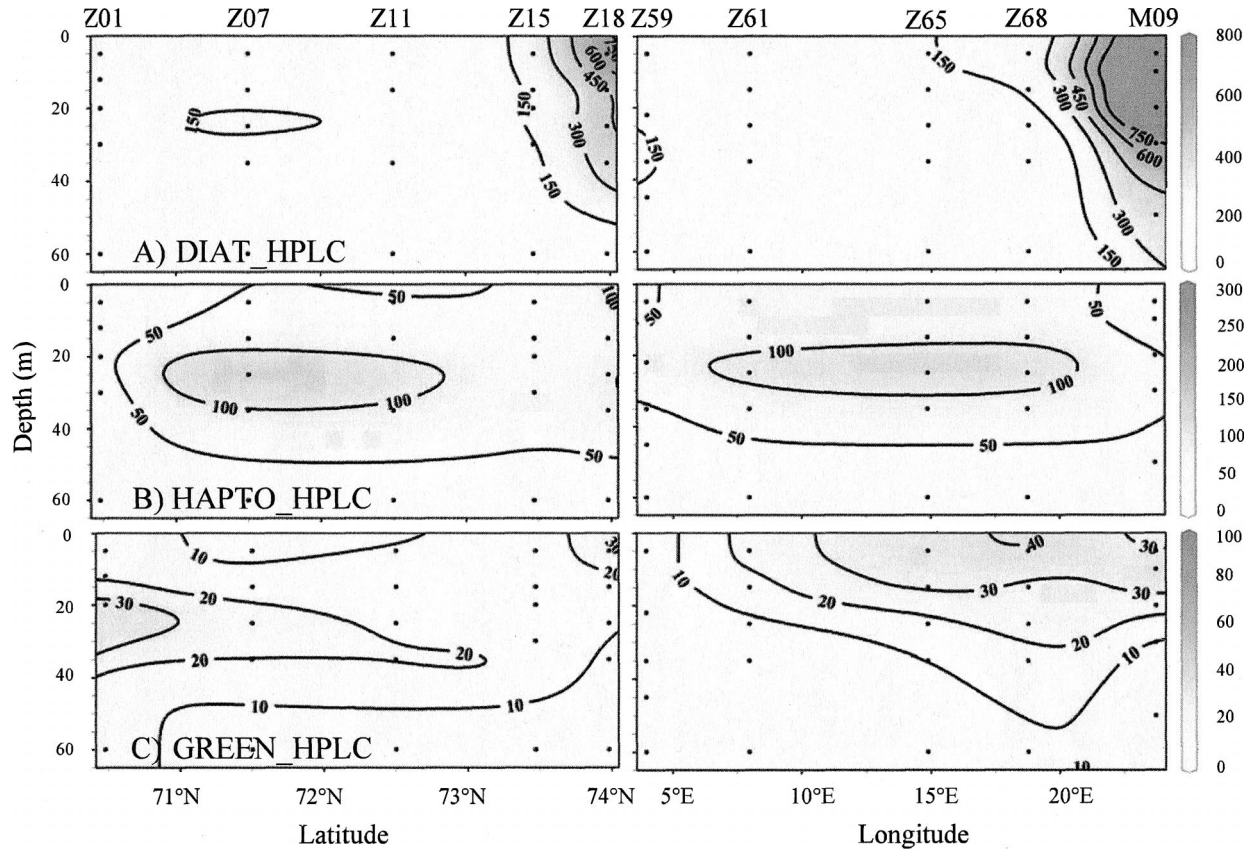

Fig. 3. Depth sections of pigment group contribution to picoplanktonic Chl *a* (ng Chl *a* L^{-1}) along the S/N and E/W transects. (A) DIAT_HPLC, (B) HAPTO_HPLC, (C) GREEN_HPLC. Black dots correspond to actual samples.

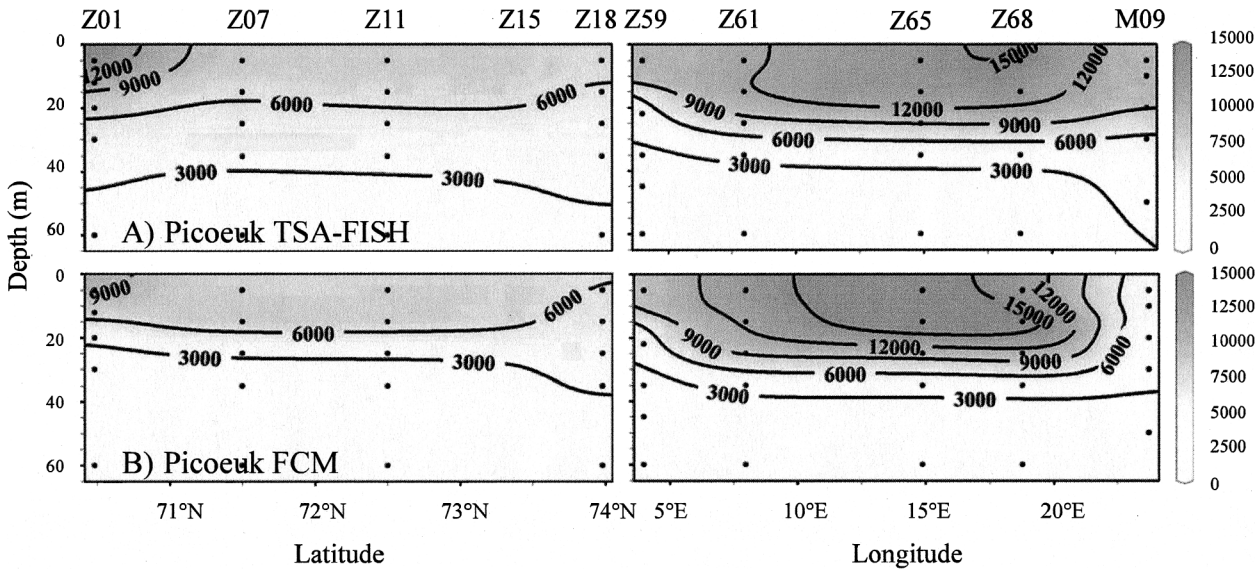

Fig. 4. Depth sections of picoeukaryote densities along the S/N and E/W transects. (A) Densities of all picoeukaryotes estimated by TSA-FISH (cells ml^{-1}). (B) Densities of photosynthetic picoeukaryotes detected by flow cytometry (cells ml^{-1}). Black dots correspond to actual samples. At Sta. Z15, samples for flow cytometry and TSA-FISH counts were not collected.

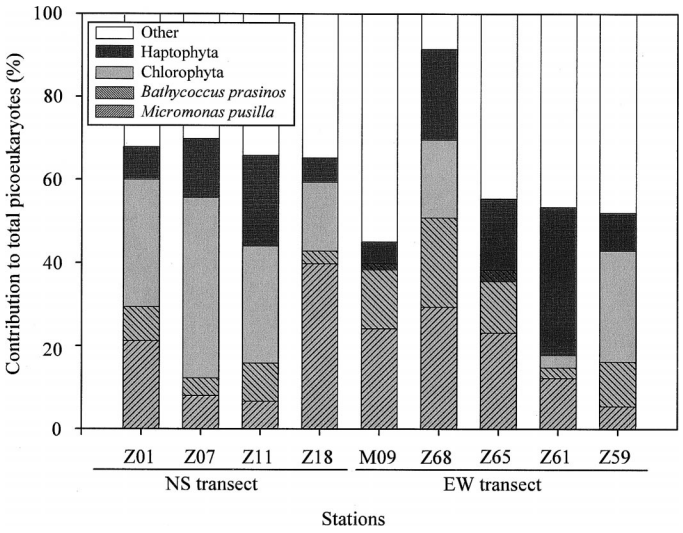

Fig. 5. Contributions of divisions Chlorophyta and Haptophyta and of the species *Micromonas pusilla* and *Bathycoccus prasinos* (both species belong to the Chlorophyta division) to the total picoeukaryotic community estimated by TSA-FISH. Contributions are expressed as percentages of the total picoeukaryotic cells. Values shown are averages calculated from the five sampled depths. At Sta. Z15, samples for TSA-FISH were not collected.

the first 30 m of the water column (Fig. 4A). In Arctic waters, picoeukaryote densities ranged between 2,600 and 10,200 cells ml^{-1}, whereas in Atlantic waters picoeukaryote densities reached a maximum of 17,000 cells ml^{-1} at Sta. Z65 (Fig. 4A). The coastal Sta. Z01 (S/N transect) showed high picoeukaryote densities as well (16,900 cells ml^{-1}).

Diversity of picoeukaryotes—Overall, 63% of the picoeukaryotes detected by TSA-FISH could be assigned to a taxon with the set of probes applied. On average, 47% of the picoeukaryotes belonged to the division Chlorophyta (Fig. 5). Their contribution to the community was maximal at Stas. Z68 and Z18 close to the polar front where they reached 70% (16,000 cells ml^{-1}) and 60% (4,400 cells ml^{-1}) of picoeukaryotes respectively, and at the coastal Sta. Z01 (60% of the picoeukaryotes) with a maximum of 9,300 cells ml^{-1} on the surface (Fig. 5). In waters with a strong Atlantic influence (Sta. Z61), their contribution was only 18%. Within the picoeukaryotic community, *M. pusilla* (Chlorophyta) was the most abundant species. In Arctic waters it represented on average 32% of the picoeukaryotes (maximum 3,200 cells ml^{-1}), 25% at stations influenced by coastal waters and those located near the polar front (Z01, Z68, and Z65, maximum 9,100 cells ml^{-1}), but only 9% at stations influenced predominantly by Atlantic waters (Z61, Z07, Z59, and Z11, Fig. 5). The species *B. prasinos* represented on average 9.3% of the picoeukaryotes in Arctic waters (maximum 1,500 cells ml^{-1}) and 11.5% in Atlantic waters (maximum 2,000 cells ml^{-1}). Stations influenced by coastal waters and at the polar front had a higher proportion of *B. prasinos* (12.6% and 18.2% of picoeukaryotes, respectively). *B. prasinos* exhibited higher cell numbers than *M. pusilla* at Sta. Z59 (Fig. 5). We did not detect any *Ostreococcus* cells in our study. The two species *B. prasinos* and *M. pusilla* accounted on average for 87% of Mamiellales cells and 60% of the Chlorophyta at Arctic and polar front stations (Fig. 5). At Stas. M09 and Z65, all the Chlorophyta cells detected could be attributed to these two species. In contrast, Chlorophyta from the stations influenced by Atlantic waters were not dominated by those species (e.g., Z61, Z11).

Cells belonging to the division Haptophyta accounted on average for 6.2% of the picoeukaryotes in Arctic waters (maximum 800 cells ml^{-1}). They were more abundant in Atlantic waters (maximum 4,500 cells ml^{-1} at Sta. Z61) where they contributed up to 35% of the picoeukaryotes at Sta. Z61 (Fig. 5). Bolidophyceae were found in all water masses but always accounted for less than 1% of the total picoeukaryotes counts (data not shown).

A good correlation was observed between cells detected by the PRYM02 probe (Haptophyta) and autotrophic cells with size 3–4 μm in the DAPI-stained preparations ($r^2 = 0.97$, $p < 0.001$, $n = 45$, $y = 0.88x - 49$) (Fig. 6A). Similarly, cells of 2 μm in size were well correlated to cells detected by probe CHLO02 targeting Chlorophyta ($r^2 = 0.83$, $p < 0.001$, $n = 45$, $y = 1.0x + 463$). This suggest that cells smaller than 2 μm observed under epifluorescence microscopy are generally chlorophytes, whereas slightly larger cells (3–4 μm) are generally haptophytes.

Discussion

Distribution of picoeukaryotic groups—The complex hydrology and the year to year variations of the location of the polar front are key characteristics of the area studied (Markowski and Wiktor 1998). In our study the abundance of cyanobacteria (i.e., *Synechococcus*) along the two transects sampled was a good indicator to discriminate between the warm Atlantic waters and the cold Arctic waters as suggested previously by Murphy and Haugen (1985) and Gradinger and Lenz (1995).

In Arctic waters, despite a moderate picoplanktonic cell density, most of the Chl *a* biomass was attributed to picoeukaryotic organisms. While more than half of the community composition was explained by the presence of Chlorophyta and Haptophyta cells (Fig. 5), pigments in the picoplanktonic fraction were largely dominated by carotenoids classically attributed to diatoms (mainly fucoxanthin) (Fig. 3).

Although one possibility would be that cell breakage took place during the filtration for size fractionation, significant contribution of fucoxanthin in the pico size fraction has been previously reported (Latasa and Bidigare 1998; Rodriguez et al. 2003). Although not observed in our samples, some diatoms (e.g., species of *Thalassiosira* Cleve, *Chaetoceros* Ehrenberg and *Arcocellus cornucervis* Hasle von Stosch and Syvertsen) may have very reduced cell size. Several pennate diatoms have slender shapes that permit them to pass through a 3-μm pore size filter. Species of *Pseudo-nitzschia* Peragallo and *Cylindrotheca closterium* (Ehrenberg) Lewin and Reiman were observed by epifluorescence in our samples, as well as in cultures established from the Arctic stations (data not shown). Indeed, at Sta. Z68, close to Arctic water, the high diatom signal could be explained by the pres-

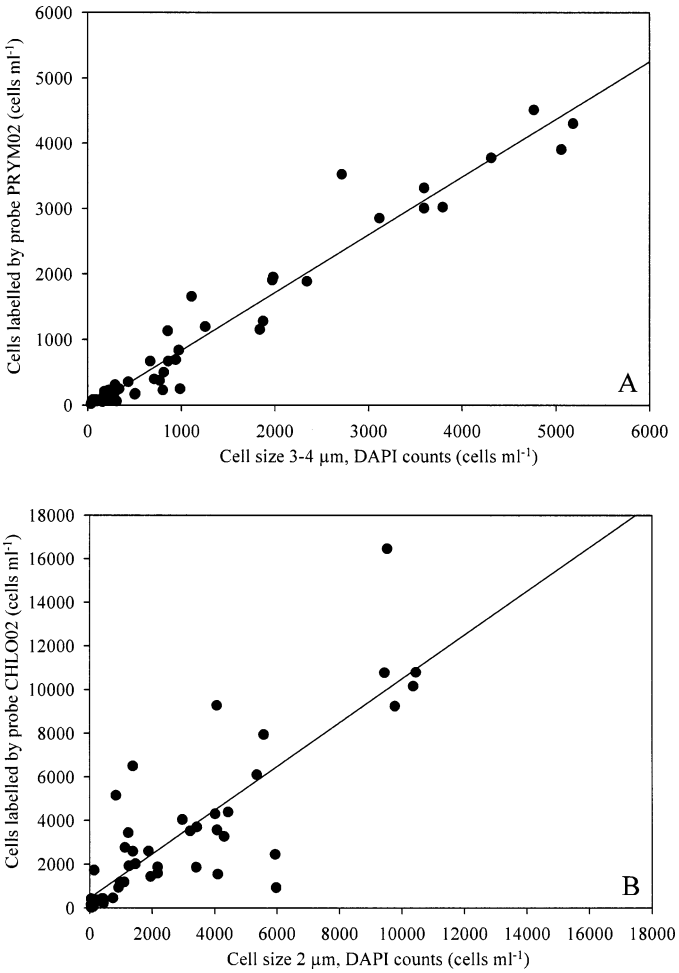

Fig. 6. (A) Correlation between DAPI counts of photosynthetic cells belonging to the size class 3–4 μm and cells detected by fluorescent in situ hybridization with the probe PRYM02 (specific for Haptophyta), $r^2 = 0.97$, $p < 0.001$, $n = 45$, $y = 0.88x - 49$. (B) Correlation between DAPI counts of photosynthetic cells of 2 μm in size and cells detected by fluorescent in situ hybridization with the probe CHLO02 (specific for Chlorophyta), $r^2 = 0.83$, $p < 0.001$, $n = 45$, $y = 1.0x + 463$.

ence at high numbers (23% of picoeukaryotes) and biomass (45% of picoeukaryotes) of these thin diatoms that would have passed through the 3-μm polycarbonate prefilter. Because of their relatively large cell volume, even a small number of these cells could then contribute disproportionately to the picoplanktonic Chl *a*. Moreover, fucoxanthin in the pico size fraction could be attributed to resting cysts of the small diatom species *Chaetoceros socialis*, which is known to form blooms in cold waters (Rat'kova and Wassmann 2002) and to produce resting spores at the end of the blooms (Owrid et al. 2000). Use of specific probes targeting diatom groups by TSA-FISH would permit clarification of this point.

Alternatively, at this time of the year, Arctic waters of the southwestern part of the Barents Sea are regulated by top-down control of microphytoplankton (Verity et al. 1999; Rat'kova and Wassmann 2002) and are known to be in a postbloom conditions (Markowski and Wiktor 1998; Owrid et al. 2000). Therefore, the high fucoxanthin values found in the pico size fraction could be due to the presence of cell debris (i.e., whole plastid outside of cells not detected by TSA-FISH) induced by zooplankton grazing. This could be the case of Sta. M09, where the low numbers of thin diatoms does not seem to explain their potentially high HPLC contribution. Furthermore the record of high levels of chlorophyllide *a* (data not shown), which is known to be a pigment marker for degraded phytoplankton and particularly diatoms (Jeffrey and Hallegraeff 1987), corroborates the existence of postbloom conditions during our sampling period in some of the samples (Stas. Z18 and M09).

In the vicinity of the polar front and in coastal waters, the situation was different since the abundance of picoeukaryotes was higher but their relative contributions to total photosynthetic biomass lower. This is probably a consequence of higher nutrient concentrations in these areas (data not shown). In Norwegian coastal waters, nutrient-rich freshwater discharges induce the phytoplankton bloom to last for several weeks into the summer (Kogeler and Rey 1999). At the polar front, the Atlantic flow and the shallow Spitsbergen bank, as well as the intense tides, have been shown to provide an almost continuous supply of nutrients south of Spitsbergen (Rat'kova and Wassmann 2002) maintaining phytoplankton growth at moderate levels throughout the summer and autumn (Kogeler and Rey 1999). Similarly, high picophytoplankton abundances corresponding to low contributions to total photosynthetic biomass have been observed previously in a wide range of oceanic conditions (Bell and Kalff 2001).

Diversity of picoeukaryotes—In our study, autotrophic cells dominated the picoeukaryotic community (75%). This is in agreement with previous studies in the Barents Sea in early summer where 70% to 80% of unidentified small flagellates (<20 μm) have been shown to be photosynthetic (Rat'kova and Wassmann 2002; Verity et al. 2002). These small flagellates (<10 μm) have been shown to be numerically important (10^3–10^4 cells ml^{-1} in Arctic waters) using serial dilution cultures, and many of these were suspected to be members of the class Prasinophyceae (Throndsen 1970). TSA-FISH investigations proved indeed that Prasinophyceae belonging to the order Mamiellales were numerically the most abundant at Arctic stations and close to the polar front.

M. pusilla was numerically the major component of the photosynthetic picoeukaryote community that we studied. It has previously been reported as prominent in the Barents Seawaters with abundances exceeding 10^4 cells ml^{-1} based on serial dilution cultures (Throndsen 1970; Throndsen and Kristiansen 1991). Moreover, *M. pusilla* has been observed to be important in various nutrient-rich waters (abundances ranging between 10^2 to 9×10^3 cells ml^{-1}), and this species is usually described as ubiquitous (Thomsen and Buck 1998; Zingone et al. 1999). Based on an average content of 0.025 pg Chl *a* per cell (DuRand et al. 2002) and TSA-FISH quantification, we estimated that this species contributed to only 7% of the picoplanktonic Chl *a* biomass in Arctic waters, although it accounted for 32% of the picoeukaryote cells. This discrepancy could be explained because other picoeukaryotic cells tend to be larger, as shown in Fig. 6, where

cells smaller than 2 μm tended to be prasinophytes, whereas cells of 3–4 μm tended to be haptophytes. In contrast, contributions to numerical abundance (25% and 9% of the picoeukaryotes) and to photosynthetic biomass (33% and 6%) were in better agreement for coastal/polar front stations and Atlantic stations, respectively. Such an important contribution to the picoplanktonic community in nutrient rich waters confirms the expected key role of *M. pusilla* in the ecology of coastal nutrient-rich waters (Not et al. 2004).

B. prasinos was recorded in Arctic waters and reached significant abundances at coastal stations and in polar front waters. Although this is the first report of *B. prasinos* from Arctic waters, its presence was expected (Throndsen and Kristiansen 1991) since it has been previously recorded from various ecosystems such as the Mediterranean sea and the western and southern coast of Norway (Eikrem and Throndsen 1990). Moreover, in spring it can reach significant abundances (1,800 cells ml^{-1}) in coastal waters of the English Channel (Not et al. 2004). *Bathycoccus*-like cells were also reported off the coast of California (Silver et al. 1986) and in the northeastern Atlantic (Johnson and Sieburth 1982).

The second most abundant group of picoplanktonic cells detected by TSA-FISH was constituted by the Haptophyta. Previous taxonomic studies in the same region, near the polar front, using microscopy and the serial dilution culture method also concluded that besides the Prasinophyceae, Haptophyta were prominent in the picoplanktonic community at this time of the year (Throndsen 1970). The highest Haptophyta abundances were detected in waters with more open ocean features (e.g., Z61, Z11). Pigment signatures of Haptophyta have also been observed to be important in the nano and pico size fraction in many oceanic regions (Moon-van der Staay et al. 2000 and references therein). In the present study, the distribution along the two transects of the pigments attributed to the Haptophyta (i.e., HAPTO_HPLC) matched convincingly with the patterns of abundances of Haptophyta detected by TSA-FISH. Indeed, according to our results, the stations with the highest haptophyte contribution to total chlorophyll *a* (for example, Stas. Z07, Z11 and Stas. Z61, Z65, Z68) also presented the highest abundances of haptophytes.

This study highlights the dominant role of a single species *Micromonas pusilla* within the picoplankton community. Clearly, further studies are necessary at the genetic, genomic, and physiological levels to understand the extraordinary dominance and the factors that drive the distribution of this organism in the environment. Another important question concerns the nature of the fucoxanthin-containing picophytoplankton: ''Can it be only explained by very small-sized diatoms and diatom debris, or are there still some groups, not yet isolated in culture and described, that contribute to this pigment signal?''

References

ANDERSON, L. G., M. CHIERICI, E. P. JONES, A. FRANSSON, AND K. OLSSON. 1998. Anthropogenic carbon dioxide in the Arctic Ocean: Inventory and sinks. J. Geophys. Res. **103:** 707–716.

BELL, T., AND J. KALFF. 2001. The contribution of picophytoplankton in marine and freshwater systems of different trophic status and depth. Limnol. Oceanogr. **46:** 1243–1248.

DURAND, M. D., R. E. GREEN, H. M. SOSIK, AND R. J. OLSON. 2002. Diel variations in optical properties of *Micromonas pusilla* (Prasinophyceae). J. Phycol. **38:** 1132–1142.

EIKREM, W., AND J. THRONDSEN. 1990. The ultrastructure of *Bathycoccus* gen. nov. and *Bathycoccus prasinos* sp. nov., a nonmotile picoplanktonic alga (Chlorophyta, Prasinophyceae) from the Mediterranean and Atlantic. Phycologia **29:** 344–350.

GIOVANNONI, S. J., E. F. DELONG, G. J. OLSEN, AND N. R. PACE. 1988. Phylogenetic group-specific oligonucleotide probes for identification of single microbial cells. J. Bacteriol. **170:** 720–726.

GRADINGER, R., AND J. LENZ. 1995. Seasonal occurrence of picocyanobacteria in the Greenland Sea and central Arctic Ocean. Polar Biol. **15:** 447–452.

GUILLOU, L., S. Y. MOON-VAN DER STAAY, H. CLAUSTRE, F. PARTENSKY, AND D. VAULOT. 1999. Diversity and abundance of Bolidophyceae (Heterokonta) in two oceanic regions. Appl. Environ. Microbiol. **65:** 4528–4536.

JEFFREY, S. W., AND G. M. HALLEGRAEFF. 1987. Chlorophyllase distribution in ten classes of phytoplankton: A problem for chlorophyll analysis. Mar. Ecol. Prog. Ser. **35:** 293–304.

JOHNSON, P. W., AND J. M. SIEBURTH. 1982. In-situ morphology and occurrence of eukaryotic phototrophs of bacterial size in the picoplankton of estuarine and oceanic waters. J. Phycol. **18:** 318–327.

KOGELER, J., AND F. REY. 1999. Ocean colour and the spatial and seasonal distribution of phytoplankton in the Barents Sea. Int. J. Remote Sens. **20:** 1303–1318.

LATASA, M., AND R. R. BIDIGARE. 1998. A comparison of phytoplankton populations of the Arabian Sea during the Spring Intermonsoon and Southwest Monsoon of 1995 as described by HPLC-analyzed pigments. Deep Sea Res. II **45:** 2133–2170.

———, K. VAN LENNING, J. L. GARRIDO, R. SCHAREK, M. ESTRADA, F. RODRIGUEZ, AND M. ZAPATA. 2001. Losses of chlorophylls and carotenoids in aqueous acetone and methanol extracts prepared for RPHPLC analysis of pigments. Chromatographia **53:** 385–391.

MACKEY, M. D., D. J. MACKEY, H. W. HIGGINS, AND S. W. WRIGHT. 1996. CHEMTAX—a program for estimating class abundances from chemical markers: Application to HPLC measurements of phytoplankton. Mar. Ecol. Prog. Ser. **144:** 265–283.

MARIE, D., C. BRUSSAARD, F. PARTENSKY, AND D. VAULOT. 1999. Flow cytometric analysis of phytoplankton, bacteria and viruses, p. 11.11.11–11.11.15. *In* J. W. Sons [ed.], Current protocols in cytometry. International Society for Analytical Cytology.

MARKOWSKI, D., AND J. WIKTOR. 1998. Phytoplankton and water masses in the European subarctic Polar front zone. Oceanologia **40:** 51–64.

MOON-VAN DER STAAY, S. Y., G. W. M. VAN DER STAAY, L. GUILLOU, D. VAULOT, H. CLAUSTRE, AND L. K. MEDLIN. 2000. Abundance and diversity of Prymnesiophytes in the picoplankton community from the equatorial Pacific Ocean inferred from 18S rDNA sequences. Limnol. Oceanogr. **45:** 98–109.

MURPHY, L. S., AND E. M. HAUGEN. 1985. The distribution and abundance of phototrophic ultraplankton in the North Atlantic. Limnol. Oceanogr. **30:** 47–58.

NOT, F., M. LATASA, D. MARIE, T. CARIOU, D. VAULOT, AND N. SIMON. 2004. A single species, *Micromonas pusilla* (Prasinophyceae), dominates the eukaryotic picoplankton in the Western English Channel. Appl. Environ. Microbiol. **70:** 4064–4072.

———, N. SIMON, I. C. BIEGALA, AND D. VAULOT. 2002. Application of fluorescent in situ hybridization coupled with tyr-

amide signal amplification (FISH-TSA) to assess eukaryotic picoplankton composition. Aquat. Microb. Ecol. **28:** 157–166.

OWRID, G., G. SOCAL, G. CIVITARESE, A. LUCHETTA, J. WIKTOR, E. NOTHIG, I. J. ANDREASSEN, U. SCHAUER, AND V. STRASS. 2000. Spatial variability of phytoplankton, nutrients and new production estimates in the waters around Svalbard. Polar Res. **19:** 155–171.

PORTER, K. G., AND Y. S. FEIG. 1980. The use of DAPI for identifying and counting aquatic microflora. Limnol. Oceanogr. **25:** 943–948.

RAT'KOVA, T. N., AND P. WASSMANN. 2002. Seasonal variation and spatial distribution of phyto- and protozooplankton in the central Barents Sea. J. Mar. Syst. **38:** 47–75.

———, ———, P. G. VERITY, AND I. J. ANDREASSEN. 1998. Abundance and biomass of pico-, nano-, and microphytoplankton on a transect across Nordvestbanken, north Norwegian shelf, in 1994. Sarsia **84:** 213–225.

RODRIGUEZ, F., Y. PAZOS, A. MORONO, J. MANEIRO, AND M. ZAPATA. 2003. Temporal variation in phytoplankton assemblages and pigment composition in a fixed station of the Ria of Pontevedra (NW Spain). Estuar. Coast. Shelf Sci. **58:** 499–515.

SCHLITZER, R. 2003. Ocean Data View. http://www.awi-bremerhaven.de/GEO/ODV.

SILVER, M. W., M. M. GOWING, AND P. J. DAVOLL. 1986. The association of photosynthetic picoplankton and ultraplankton with pelagic detritus through the water column (0–200 m), p. 311–341. *In* T. Platt and W. K. W. Li [eds.], Photosynthetic picoplankton. Canadian Bulletin of Fisheries and Aquatic Sciences.

SIMON, N., L. CAMPBELL, E. ORNOLFSDOTTIR, R. GROBEN, L. GUILLOU, M. LANGE, AND L. K. MEDLIN. 2000. Oligonucleotide probes for the identification of three algal groups by dot blot and fluorescent whole-cell hybridization. J. Eukaryot. Microbiol. **47:** 76–84.

———, N. LEBOT, D. MARIE, F. PARTENSKY, AND D. VAULOT. 1995. Fluorescent in situ hybridization with rRNA-targeted oligonucleotide probes to identify small phytoplankton by flow cytometry. Appl. Environ. Microbiol. **61:** 2506–2513.

THOMSEN, H. A., AND K. R. BUCK. 1998. Nanoflagellates of the central California waters: Taxonomy, biogeography and abundance of primitive, green flagellates (Pedinophyceae, Prasinophyceae). Deep-Sea Res. II **45:** 1687–1707.

THRONDSEN, J. 1970. Flagellates from Arctic waters. Nytt Magasin Bot. **17:** 49–57.

———, AND S. KRISTIANSEN. 1991. *Micromonas pusilla* (Prasinophyceae) as part of pico- and nanoplankton communities of the Barents Sea. Polar Res. **10:** 201–207.

VAULOT, D. 1989. CYTOPC: Processing software for flow cytometric data. Signal and Noise **2:** 8.

VERITY, P. G., P. WASSMANN, M. E. FRISCHER, M. N. HOWARD-JONES, AND A. E. ALLEN. 2002. Grazing of phytoplankton by microzooplankton in the Barents Sea during early summer. J. Mar. Syst. **38:** 109–123.

———, ———, T. N. RAT'KOVA, I. J. ANDREASSEN, AND E. NORDBY. 1999. Seasonal patterns in composition and biomass of autotrophic and heterotrophic nano- and microplankton communities on the north Norwegian shelf. Sarsia **84:** 265–277.

ZAPATA, M., F. RODRIGUEZ, AND J. L. GARRIDO. 2000. Separation of chlorophylls and carotenoids from marine phytoplankton: A new HPLC method using a reversed phase C-8 column and pyridine-containing mobile phases. Mar. Ecol. Prog. Ser. **195:** 29–45.

ZINGONE, A., D. SARNO, AND G. FORLANI. 1999. Seasonal dynamics in the abundance of *Micromonas pusilla* (Prasinophyceae) and its viruses in the Gulf of Naples (Mediterranean Sea). J. Plankton Res. **21:** 2143–2159.

Received: 28 October 2004
Accepted: 28 March 2005
Amended: 25 April 2005